A REGULARIZED CONJUGATE GRADIENT METHOD FOR WAVE FIELD TRANSFORMATION OF TRANSIENT ELECTROMAGNETIC FIELD

Guo Fu WANG [1], Xiao Yu ZHAO [2*], Jin Cai YE [3,] Fa Quan ZHANG[4]

The wave field transformation is a useful way of achieving pseudo-seismic interpretation for transient electromagnetic (TEM) method. But the equation in the wave field transformation belongs to the first-class Fredholm integration equation, which is a very ill-posed inverse problem. Considering that the conjugate gradient (CG) method is quite efficient for solving a symmetric positive definite (SPD) system of linear equations whose coefficient matrix has tightly clustered spectrum, in this paper, a new pre-conditioned regularized conjugate gradient (PRCG) method is proposed to realize the full-domain wave field transformation from diffusion equation to wave equation. The SSOR pre-conditioned process significantly reduces the condition number of the coefficient matrix, and regularization improves the spectral properties of the coefficient matrix, while the CG iteration helps run the transformation of wave field in full time-domain. The comparison between the transform results and the known wave field functions shows that the algorithm is stable and reliable. Comparison of the results with the results of the regularized conjugate gradient method and pre-existing PRCG method show that the algorithm proposed in this paper converges faster, and more stable.

Keywords: Transient electromagnetic (TEM); wave field transformation; regularized conjugate gradient method; pre-conditioned conjugate gradient method

1. Introduction

The transient electromagnetic method (TEM) has a broad application prospect and great development potential in the fields of solid mineral, oil and gas resources and hydraulic environment exploration [1-5]. TEM pseudo-seismic interpretation technique is an effective means to achieve 3D inversion of transient

[1] School of Information and Communication, Guilin University of Electronic Technology, Guilin 541004, China; e-mail: guofwang@126.com
[2*] School of Information and Communication, Guilin University of Electronic Technology, Guilin 541004, China; e-mail: zhaoxiaoyu588@126.com
[3] School of Information and Communication, Guilin University of Electronic Technology, Guilin 541004, China; e-mail: kingsey@126.com
[4] School of Information and Communication, Guilin University of Electronic Technology, Guilin 541004, China; e-mail: zhangfq@guet.edu.cn

electromagnetic data. One of the key problems is to realize the transformation from transient electromagnetic fields to fictitious wave fields.

As early as 1972, Kunetz studied the *magnetotelluric* (MT) interpretation and inversion in layered media and found that there is an interesting similarity between MT field and its corresponding diffusion equation with seismic wave field and wave equation [6]. Lavrent'ev deduced the mathematical integral relationship between the electromagnetic field and fictitious wave field in 1986 [7]. The results of Lee's research in 1989 show that this relationship is also applicable to vector electromagnetic fields [8]. However, due to wave field transformation equations belong to the first-class Fredholm integration equation, which is a very ill-posed inverse problem. In order to improve the ill-posed of the wave-field transformation, Chen et al. realized the wave field transformation by using *singular value decomposition* (SVD) algorithm [9]. Later, Li et al. achieved the transformation from transient electromagnetic field to wave field by using regularization algorithm. To ensure that the conditional number of coefficient matrix was not too large, the signals of transient electromagnetic field in time domain was divided into seven segments for calculation, which effectively reduced the ill-posed degree of the matrix, but it also introduced the problem of the link between segment and segment [4, 10]. In addition, several studies have made fruitful and meaningful works on the application of the transformed wave field [4, 5, 11, 12]. However, there are still many problems in this field, and finding a stable and reliable wave field transformation algorithm is the focus of the research.

In this paper, the new pre-conditioned conjugate gradient method (PRCG) is used to realize the full time domain wave field transformation, which not only avoids the segmentation effectively, but also realizes the transformation between the transient electromagnetic field satisfying the diffusion equation and the wave field satisfying the wave equation.

2. Theory of the wave field transformation

The time domain TEM belongs to low frequency detection technologies, and this frequency required are usually less than 30 kHz, and for typical earth conductivities, the conduction current is several orders of magnitude greater than the displacement current, and the displacement current is usually negligible [8].

In a conductive medium, the electric and magnetic fields satisfy the following diffusion equations while the displacement current is ignored, respectively.

$$\nabla \times \nabla \times \boldsymbol{E}(\boldsymbol{r}, \mathrm{t}) + \mu_0 \sigma(\boldsymbol{r}) \frac{\partial}{\partial t} \boldsymbol{E}(\boldsymbol{r}, t) = \boldsymbol{S}_E(\boldsymbol{r}, t) \tag{1}$$

$$\nabla \times \nabla \times \boldsymbol{H}(\boldsymbol{r},\mathrm{t}) + \mu_0 \sigma(\boldsymbol{r}) \frac{\partial}{\partial t} \boldsymbol{H}(\boldsymbol{r},t) = \boldsymbol{S}_H(\boldsymbol{r},t) \tag{2}$$

where $\boldsymbol{S}_E(\boldsymbol{r},t)$ and $\boldsymbol{S}_H(\boldsymbol{r},t)$ are the source terms corresponding to the electric field diffusion equation (1) and the magnetic field diffusion equation (2) respectively.

The functions $\boldsymbol{U}_E(\boldsymbol{r},\mathrm{q})$ and $\boldsymbol{S}_{U_E}(\boldsymbol{r},\mathrm{q})$ are introduced to satisfy the following wave equations:

$$\nabla \times \nabla \times \boldsymbol{U}_E(\boldsymbol{r},\mathrm{q}) + \mu_0 \sigma(\boldsymbol{r}) \frac{\partial^2}{\partial t^2} \boldsymbol{U}_E(\boldsymbol{r},q) = \boldsymbol{S}_{U_E}(\boldsymbol{r},q) \tag{3}$$

Combining the equations (1) and (3), we see that the variable q is independent and has the dimension of square root of time. The function $\boldsymbol{U}_E(\boldsymbol{r},\mathrm{q})$ would behave as if it were a propagating wave with a velocity of $(\mu_0\sigma)^{-1/2}$ in $\mathrm{m}/\sqrt{\mathrm{s}}$.

Laplace transforming equations (1) and (3) from t to s and from q to p, respectively, we obtain the equations as the following

$$\nabla \times \nabla \times \hat{\boldsymbol{E}}(\boldsymbol{r},\mathrm{s}) + \mu_0 \sigma(\boldsymbol{r}) s\hat{\boldsymbol{E}}(\boldsymbol{r},s) = \hat{\boldsymbol{S}}_E(\boldsymbol{r},s) \tag{4}$$

and

$$\nabla \times \nabla \times \hat{\boldsymbol{U}}_E(\boldsymbol{r},p) + \mu_0 \sigma(\boldsymbol{r}) P^2 \hat{\boldsymbol{U}}_E(\boldsymbol{r},p) = \hat{\boldsymbol{S}}_{U_E}(\boldsymbol{r},p) \tag{5}$$

If we let $s = p^2$, then equation (4) becomes

$$\nabla \times \nabla \times \hat{\boldsymbol{E}}(\boldsymbol{r},p^2) + \mu_0 \sigma(\boldsymbol{r}) p^2 \hat{\boldsymbol{E}}(\boldsymbol{r},p^2) = \hat{\boldsymbol{S}}_{\mathrm{E}}(\boldsymbol{r},p^2) \tag{6}$$

Combining equations (5) and (6), under an additional condition $\hat{\boldsymbol{S}}_E(\boldsymbol{r},p^2) = \hat{\boldsymbol{S}}_{U_E}(\boldsymbol{r},p)$, we obtain the following equation

$$\hat{\boldsymbol{E}}(\boldsymbol{r},p^2) = \hat{\boldsymbol{U}}_E(\boldsymbol{r},\mathrm{p})$$

This result implies, after removing space variable $\boldsymbol{r}$, that

$$\int_0^\infty \boldsymbol{E}(t) e^{-p^2 t} dt = \int_0^\infty \boldsymbol{U}_E(q) e^{-pq} dq$$

Because of $s = p^2$, we have

$$\int_0^\infty \boldsymbol{E}(t) e^{-st} dt = \int_0^\infty \boldsymbol{U}_E(q) e^{-\sqrt{s}q} dq$$

Using inverse Laplace transforming (from s to t) both sides of the last equation, we eventually obtain the integral relation between the electric field $\boldsymbol{E}(\mathrm{t})$ and the corresponding wave field $\boldsymbol{U}_E(\mathrm{q})$, as the following equation

$$\boldsymbol{E}(t) = \frac{1}{2\sqrt{\pi t^3}} \int_0^\infty q e^{-q^2/4t} \boldsymbol{U}_E(q) \mathrm{d}q \tag{7}$$

In the same way, we introduce the functions $\boldsymbol{U}_H(\boldsymbol{r},\mathrm{q})$ and $\boldsymbol{S}_{U_H}(\boldsymbol{r},\mathrm{q})$, which represent the wave field corresponding to the magnetic field and its source term, respectively. Similarly, if we make $\hat{\boldsymbol{S}}_H(\boldsymbol{r},p^2)=\hat{\boldsymbol{S}}_{U_H}(\boldsymbol{r},p)$, the integral relation between the magnetic field $\boldsymbol{H}(\mathrm{t})$ and the corresponding wave field $\boldsymbol{U}_H(\mathrm{q})$ can be derived from the diffusion equation (2).

$$\boldsymbol{H}(t)=\frac{1}{2\sqrt{\pi t^3}}\int_0^\infty qe^{-q^2/4t}\boldsymbol{U}_H(q)\mathrm{d}q \tag{8}$$

The induced electromotive force (the rate of change of magnetic induction intensity with time) is usually collected when the TEM method is used for geological exploration. By $\boldsymbol{B}=\mu_0\boldsymbol{H}$, we have

$$\frac{\partial\boldsymbol{B}(t)}{\partial t}=\frac{1}{2\sqrt{\pi t^3}}\int_0^\infty \mu_0 q(\frac{q^2}{4t^2}-\frac{3}{2t})e^{-q^2/4t}\boldsymbol{U}_B(q)\mathrm{d}q \tag{9}$$

The equations (7), (8) and (9) are the transformation from wave fields to diffusion fields, which are called a direct problem. Inversely, the diffuse field is known to be the wave field and called an inverse problem that is usually ill-posed. These transformations, involving only t and q, are independent of $\boldsymbol{r}$.

From these transformations and their derivation process, we find that the wave field transformation is unconfined to the form of the transient electromagnetic response, and applicable to multiple transient electromagnetic field components.

3. Numerical algorithm for wave field transformation

The wave field transformation equations (7) (8) and (9) are discretized and rewritten into a unified numerical integral form

$$f(t_i)=\sum_{j=1}^{n}u(q_j)a(t_i,q_j)\Delta q_j \tag{10}$$

where $f(t_i)$ is the transient electromagnetic field, which can be electric field, magnetic field or induced electromotive force. The term $a(t_i,q_j)$ is the kernel function, for equations (7) and (8), $a(t_i,q_j)=q_je^{-q_j^2/4t_i}\Big/(2\sqrt{\pi t_i^3})$, while for equation (9), $a(t_i,q_j)=q\left(q^2/4t_i^2-3/2t_i\right)e^{-q^2/4t_i}\Big/(2\sqrt{\pi t_i^3})$. Here, Δq_j is the integral coefficient.

The discretized equation (10) is considered as a linear inverse problem

$$Ax=b \tag{11}$$

where the coefficient matrix $A \in R^{m \times n}$ contains the kernel function $a(t_i, q_j)$ and the integral coefficient Δq_j, and $x \in R^n$ is the wave field values to be solved, and b is the known transient electromagnetic field data.

Considering that *conjugate gradient* (CG) methods are quite efficient for solving symmetric positive definite systems of linear equations, of which coefficient matrices have tightly clustered spectra, a new *regularized conjugate gradient* (RCG) method can be used in the case for solving the system of linear equations.

Premultiply matrix A^T on both sides of equation (11)

$$A^T A x = A^T b \tag{12}$$

If A is a full rank matrix (row full rank or column full rank), then $A^T A$ is a symmetric positive definite matrix.

We use $v = \dfrac{\mu}{\eta}$ to represent the horizontal intercept of the linear transformation $f : R^1 \to R^1$,

$$f(t) = \mu + \eta t \,,\ \mu, \eta \in R^1, \quad \eta \neq 0 \tag{13}$$

Evidently, for a symmetric positive definite matrix $A^T A$, $f(A^T A) = \eta A(v)$ where $A(v) = vI + A^T A$ is a transformation matrix and I is a unit matrix. The linear transformation (13) maps the spectral set $\sigma(A)$ of the matrix $A^T A$ into a new set $f(\sigma(t)) = \mu + \eta\sigma(A^T A)$. If we choose the reals μ, η, of which $\eta \neq 0$ and $v > 0$, it holds that

$$\kappa_2(f(A^T A)) \equiv \frac{\mu + \eta\lambda_{\max}(A^T A)}{\mu + \eta\lambda_{\min}(A^T A)} = \frac{v + \eta\lambda_{\max}(A^T A)}{v + \eta\lambda_{\min}(A^T A)} < \frac{\lambda_{\max}(A^T A)}{\lambda_{\min}(A^T A)} \equiv \kappa_2(A^T A)$$

The condition number $\kappa(A^T A)$ of coefficient matrix $A^T A$ with respect to the Euclidean norm is given by $\kappa(A^T A) = \left\| A^T A \right\|_2 \left\| (A^T A)^{-1} \right\|_2 = \dfrac{\lambda_{\max}(A^T A)}{\lambda_{\min}(A^T A)}$. Therefore, linear transformation (13) can reduce the condition number of coefficient matrix $A^T A$. The constant μ is called a shift, and the constant η as a contractor, when $|\eta| < 1$ and an amplifier when $|\eta| > 1$.

By the linear transformation (13), we rewrite the system of linear equations (12) as

$$(vI + A^T A)x = vx + A^T b \tag{14}$$

where $I \in R^{n \times n}$ is an identity matrix, and $v > 0$ that is called as a regularization parameter. Therefore, the system of the linear equations (14) is an equivalent system of the linear equations (12).

In order to further reduce the condition number $\kappa_2(A(v))$ of the coefficient matrix $A(v)$ of the regularized linear system (14), and improve the performance of the method, we can pre-condition the regularized linear system (14). *Symmetric successive over-relaxation* (SSOR) preconditioning is quite efficient method to reduce the condition number of coefficient matrix [13-15]. It has been proved that after preconditioning, the matrix has the condition number of the original square root [13]. In addition, one SSOR preconditioner is obtained easily in the following [16, 17].

By decomposing the matrix $A(v)$ into its lower triangular part L, its diagonal part D, and its upper triangular part L^T, i.e.,

$$A(v) = L + D + L^T .$$

Then, the SSOR preconditioner

$$M(v) = \frac{1}{\omega(2-\omega)}\left[(D+\omega L)^{-1} D^{-1} (D+\omega L^T)\right].$$

Then the eigenvalues of the matrix $M(v)^{-1}A(v)$ will be clustered near one, thus accelerating the convergence rate of the CG iteration.

The above description of the process suggests the following *pre-conditioned regularized conjugate gradient* (PRCG) method:

1. *The linear system* $A^T Ax = A^T b$ *is obtained by premultiply matrix* A^T.
2. *The linear system* $A^T Ax = A^T b$ *is first regularized by reasonably shifting and contracting the spectrum of the coefficient matrix* $A^T A$, *then we have the regularized linear system* $(vI + A^T A)x = vx + A^T b$.
3. *Preconditioning the regularized linear system* $(vI + A^T A)x = vx + A^T b$ *by the SSOR preconditioner* $M(v)$, *and we have the pre-conditioned regularized linear system* $M(v)^{-1}(vI + A^T A)x = M(v)^{-1}(vx + A^T b)$.
4. *Supposing we have got approximations* $x^{(1)}, x^{(2)}, ..., x^{(k)}$ *to the solution* x^* *of the system of linear equation (11) under a given starting vector* $x^{(0)} \in R^n$, *then the next approximation* $x^{(k+1)}$ *to* x^* *is obtained through solving the system of linear equations*

$$M(v)^{-1}(vI + A^T A)x^{(k+1)} = M(v)^{-1}(vx^{(k)} + A^T b) \qquad (15)$$

Iteratively, with the CG method, to certain arithmetic precision.

4. Numerical examples and fictitious wave field analysis

In this section, we transform the transient electromagnetic responses of uniform half-space model and layered geoelectric models into the corresponding fictitious wave fields to assess performance of the PRCG method proposed in this

paper. Considering that the transient electromagnetic field components ($E(t)$, $H(t)$ and $B'(t)$) have the same wave field transformation form, we take the magnetic field $H(t)$ as an example of wave field transformation.

4.1 Wave field transformation of response on uniform half-space model

To verify the correctness of the wave field transformation algorithm, we take the theoretical value of the wave field as $U(q)=1$. Directly integrating Eq. (8), transient electromagnetic response attenuation curve is obtained, as shown in Fig. 1(a). The shape of the transient electromagnetic response attenuation curves is consistent with the variation of the attenuation curve of the forward in uniform half-space geoelectric model. It can be assumed that the constant wave field $U(q)=1$ is the wave function of the uniform half-space geoelectric model.

For comparison, the wave field transformation result obtained by the RCG method is shown in Fig. 1(b), and Fig. 1 (c) shows the wave field transformation results obtained by the PRCG method. It is easily found that the algorithm after SSOR preconditioning converges much better than that without preconditioning and protects from the case of non-convergence. This is due to that SSOR pre-conditioned greatly reduces the condition number of coefficient matrix and the ill-conditioned degree of the equation. However, the regularization algorithm adopted in the literature [4, 7] does not perform precondition processing. It is necessary to adopt a processing method of segmenting the transient electromagnetic time signal to reduce the condition number of the coefficient matrix in the process of the wave field transform. Here, the PRCG method realizes the full-time wave field transformation without segmenting signal while avoiding connection problems among different segments.

Fig. 1(d) shows the wave field transform results using Qi's PRCG method (Ref. [13]) with the same parameters. Compared with the results of the PRCG method proposed in this paper (Fig. 1(c)), Qi's PRCG algorithm result converge relatively slower. In addition to the small fluctuations in the beginning stages, subsequently there are some subtle fluctuations. Table 1 shows the comparison of the wave field transformation results between the PRCG method and Qi's PRCG method with the same parameters.

Table 1

Comparison of wave field transformation results between PRCG method and Qi's PRCG method with the same parameters

	Outer iteration steps	Total iteration steps	Time (s)	Error (%)
PRCG method	5	116	0.011262	1.979
Qi's PRCG	1000	24449	3.668706	2.8919

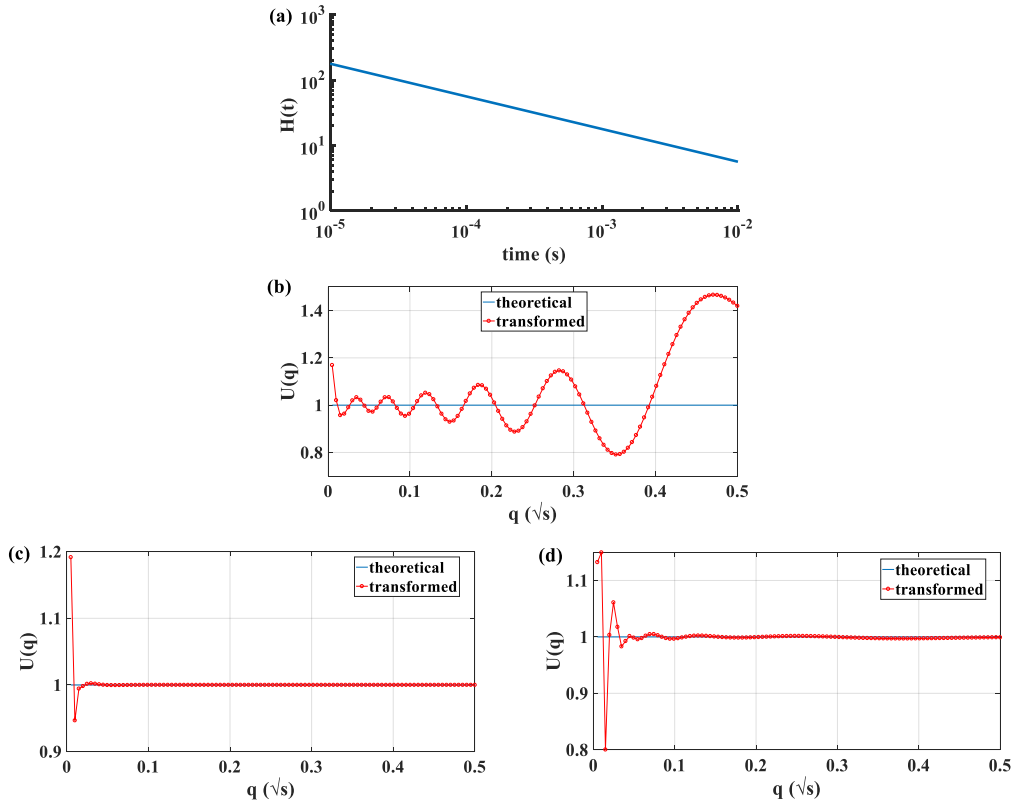

(a) Transient electromagnetic response attenuation curve
(b) The wave field transformation result with the RCG method
(c) The wave field transformation result with the PRCG method
(d) The wave field transformation result with Qi's PRCG method
Fig.1. Comparison of wave field transformation results between the RCG method, PRCG method and Qi's PRCG method

4.2 Wave field transformation of response on two-layer model

The stability and reliability of the method is illustrated by the constant wave field $U(q)=1$ above. In order to further test the performance of the proposed method, the PRCG method is used to transform the transient electromagnetic response of the two-layer geoelectric model.

Adding a Gaussian pulse and on the basis of the constant wave field $U(q)=1$, the wave function of two-layer geoelectric model is shown in the following equation:

$$U(q)=1+\alpha\cdot e^{-4\pi(q-q_0)^2/\beta^2} \tag{16}$$

where α, β and q_0 are the amplitude, width and time delay of pulse, respectively.

4.2.1 Single positive pulse wave field

In this model, let the parameters $\alpha = 2\sqrt{s}$, $\beta = 0.04\sqrt{s}$, and $q_0 = 0.05\sqrt{s}$. Directly integrating Eq. (8), corresponding transient electromagnetic response attenuation curve is obtained, as shown in Fig. 2(a). The shape of the transient electromagnetic field attenuation curve in the figure is consistent with the variation of the attenuation curve of the forward in D-type geoelectric model ($\rho_1 > \rho_2$, of which ρ_1 is the resistivity of the first layer of the model, and ρ_2 is the resistivity of the second layer). Assuming that the single positive pulse wave field is the wave function of D-type geoelectric model, we conclude that the peak time, width, and polarity of the pulse correspond respectively to the interface of electrical, resistivity difference, and relative variation between the high and low resistivity of geoelectric model (amplitude is positive, when $\rho_1 > \rho_2$, and negative when $\rho_1 < \rho_2$).

Using the PRCG method, we realized the wave field transformation for the transient electromagnetic field in Fig. 2(a), and result are shown in Fig. 2(b). From the result, we find that the transformed solution complies with the theoretical solution. To verify the stability of the algorithm, we add respectively 3% and 5% noise to the transient electromagnetic field in Fig. 2(a), while increasing the value of regularization parameter v in the calculation. The transient electromagnetic field data after the addition of the noise and the corresponding wave field transformation results are shown in Fig. 3 and Fig. 4. The analysis shows that the resolution of the solution is reduced due to the increase of the value of the regularized parameter v, but transformed solutions are still very stable.

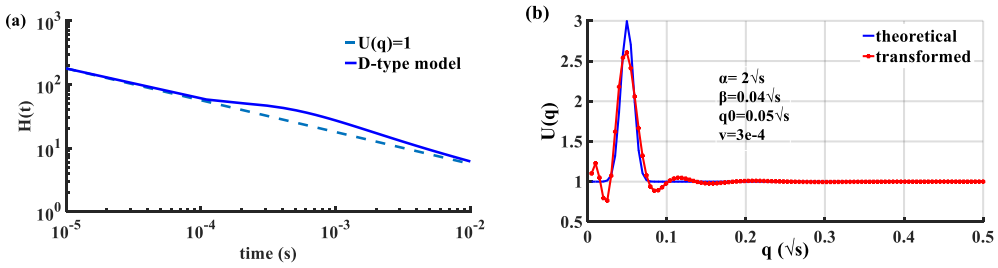

(a) Transient electromagnetic response attenuation curve
(b) Comparison of the transformed and theoretical solutions ($v = 3e-4$)
Fig. 2. Comparison of the transformed and theoretical solutions for the wave field $U(q)$ in the q domain on the D-type geoelectric model.

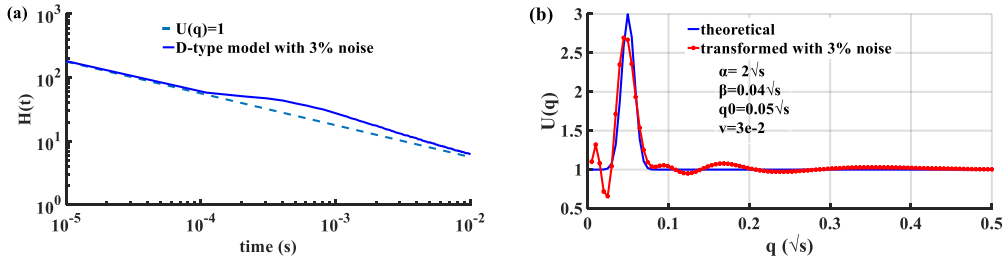

(a) Transient electromagnetic response attenuation curve (with 3% noise)

(b) Comparison of the transformed and theoretical solutions (with 3% noise, $v = 3e-2$)

Fig. 3. Comparison of the transformed and theoretical solutions for the wave field $U(q)$ in the q domain on the D-type geoelectric model.

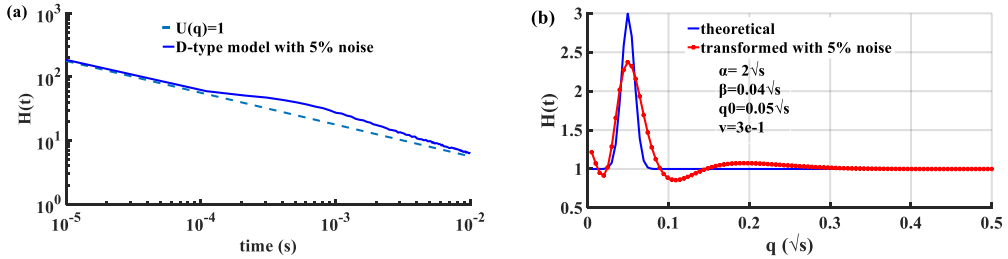

(a) Transient electromagnetic response attenuation curve (with 5% noise)

(b) Comparison of the transformed and theoretical solutions (with 5% noise, $v = 3e-1$)

Fig. 4. Comparison of the transformed and theoretical solutions for the wave field $U(q)$ in the q domain on the D-type geoelectric model.

4.2.2 Single negative pulse wave field

In this model, let the parameters $\alpha = -2\sqrt{s}$, $\beta = 0.04\sqrt{s}$, and $q_0 = 0.05\sqrt{s}$. Directly integrating Eq. (8), corresponding transient electromagnetic response attenuation curve is obtained, as shown in Fig. 5(a). The shape of the transient electromagnetic field attenuation curve in the figure is consistent with the variation of the attenuation curve of the forward in G-type geoelectric model ($\rho_1 < \rho_2$). Similarly, assuming that the single negative pulse wave field are recorded as the wave function of G-type geoelectric model, and using the PRCG method, the wave field transformation results for the transient electromagnetic field in Fig. 5(a) are shown in Fig. 5(b). Similarly, adding respectively 3% and 5% noise to the transient electromagnetic field in Fig. 5(a), and increasing the value of regularization parameter v in the calculation, we obtain results shown in Fig. 5(c) and Fig. 5(d).

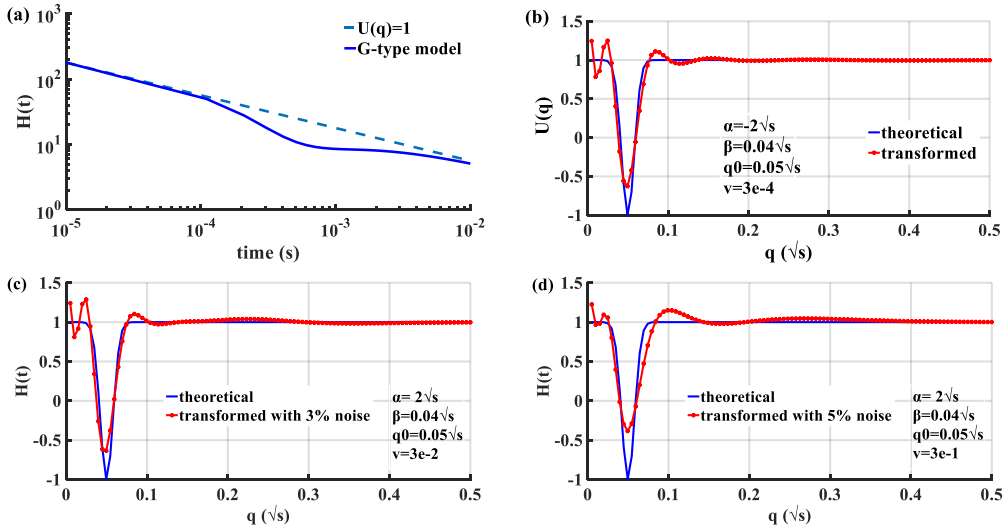

(a) Transient electromagnetic response attenuation curve

(b) Comparison of the transformed and theoretical solutions ($v = 3e-4$)

(c) Comparison of the transformed and theoretical solutions (with 3% noise, $v = 3e-2$)

(d) Comparison of the transformed and theoretical solutions (with 5% noise, $v = 3e-1$)

Fig. 5. Comparison of the transformed and theoretical solutions for the wave field $U(q)$ in the q domain on the G-type geoelectric model.

4.3 Wave field transformation of response on three-layer model

In geoelectric exploration, the influence of interlayer reflection and multiple reflection of monolayer in the media, the extraction and recognition of effective information in multi-layer geoelectric interface have unexpectable challenges. For solving the difficulties, researchers have developed innovated algorithms in data processing and data interpretation, such as stack technique, de-convolution technique, and other techniques, aiming to improve the longitudinal resolution. For fictitious wave field, it is far difficult to extract and identify geoelectric interface information due to the propagation speed and significantly attenuation of wave field. In this section, the wave field transformation results of the transient electromagnetic response of the typical Q, A, H, K three-layer geoelectric model are given in order to get some further understanding of fictitious wave field.

On the basis of two-layer model, the wave function of three-layer geoelectric model is given by adding a Gaussian pulse, as shown in Eq. (17).

$$U(q) = 1 + \alpha_0 \cdot e^{-4\pi(q-q_0)^2/\beta_0^2} + \alpha_1 \cdot e^{-4\pi(q-q_1)^2/\beta_1^2} \tag{17}$$

where α_0 , β_0 and q_0 denote the amplitude, width and peak time of the first pulse respectively, and α_1 , β_1 and q_1 denote the parameters of the second pulse.

In this model, let the parameters $\alpha_0 = \pm 2\sqrt{s}$, $\beta_0 = 0.03\sqrt{s}$, $q_0 = 0.03\sqrt{s}$ and $\alpha_1 = \pm 2\sqrt{s}$, $\beta_1 = 0.03\sqrt{s}$, $q_1 = 0.12\sqrt{s}$. Directly integrating Eq. (8), corresponding transient electromagnetic response attenuation curves are obtained, as shown in Figs. 6(a), 7(a), 8(a) and 9(a), and wave field transformation results are shown in Figs. 6(b), 7(b), 8(b) and 9(b), respectively. The analysis shows that the shorter duration of wavelet leading to the higher amplitude of wavelet, the resolution of range is higher. While the propagation distance or propagation time is increased, the amplitude of the wavelet is decreased gradually by the filtering of the earth, and the width of the wavelet is broadened, so that the resolution of the range decreases. As we know, the loss of the high-frequency component is greater than that of the low-frequency component.

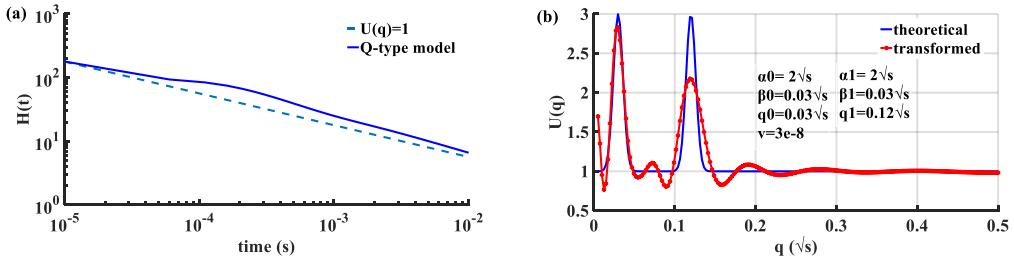

(a) Transient electromagnetic response attenuation curve
(b) Comparison of the transformed and theoretical solutions ($v = 3e-8$)
Fig. 6. Comparison of the transformed and theoretical solutions for the wave field $U(q)$ in the q domain on the Q-type geoelectric model.

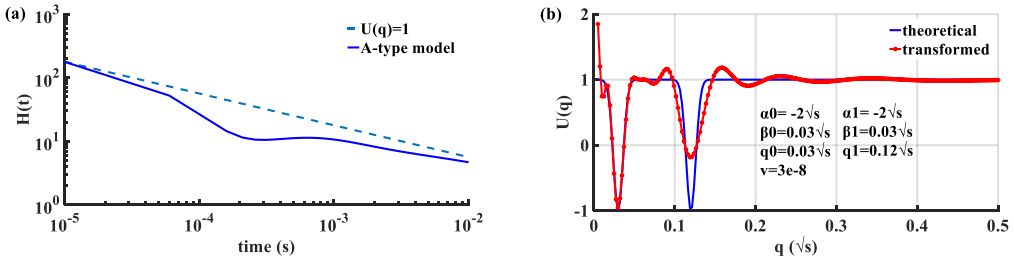

(a) Transient electromagnetic response attenuation curve
(b) Comparison of the transformed and theoretical solutions ($v = 3e-8$)
Fig. 7. Comparison of the transformed and theoretical solutions for the wave field $U(q)$ in the q domain on the A-type geoelectric model.

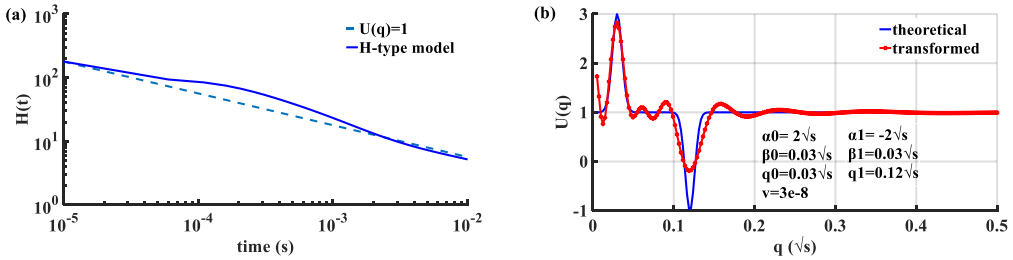

(a) Transient electromagnetic response attenuation curve

(b) Comparison of the transformed and theoretical solutions ($v = 3e-8$)

Fig. 8. Comparison of the transformed and theoretical solutions for the wave field $U(q)$ in the q domain on the H-type geoelectric model.

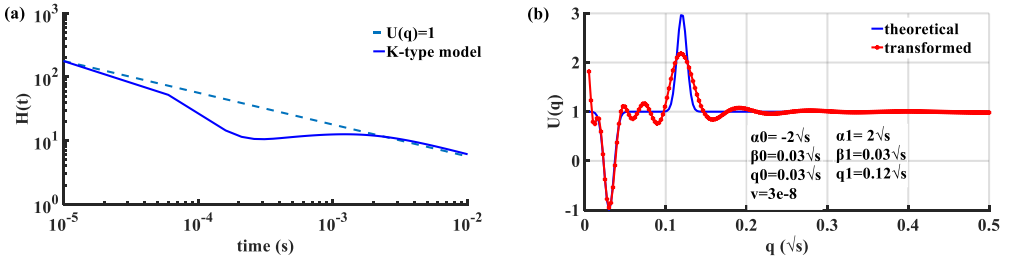

(a) Transient electromagnetic response attenuation curve

(b) Comparison of the transformed and theoretical solutions ($v = 3e-8$)

Fig. 9. Comparison of the transformed and theoretical solutions for the wave field $U(q)$ in the q domain on the K-type geoelectric model.

5. Conclusion

In this work, we investigate the numerical calculation method from electromagnetic diffusion field to fictitious wave field. By deriving and implementing the transformation between the transient electromagnetic field, satisfying the diffusion equation, and the fictitious "wave field", satisfying the wave equation, we obtain mathematically "the fluctuation" of the electromagnetic field in the induction region. Thus, the decay curve of the transient electromagnetic field with time is transformed stably and effectively into its corresponding wave propagation curve of fictitious "wave field" with time-like. Firstly, the algorithm is verified by the constant wave field, which proves that the method is stable and reliable. Then, using the algorithm developed in the paper, the transient electromagnetic responses of the two-layer geoelectric model are transformed into corresponding wave fields. The Gaussian pulse is used as the wavelet to synthesize the wave function, and the geoelectric model is simulated to illustrate the effect of the proposed algorithm. The wave field transformation of the response of the three-layer geoelectric model shows the applicability of the proposed algorithm to the complex model.

Acknowledgments

This work is supported by the National Natural Science Foundation of China under Grant number 61761009.

R E F E R E N C E S

[1]. *G.Q. Xue, W.Y, Chen, S. Yan,* Research study on the short offset time-domain electromagnetic method for deep exploration. Journal of Applied Geophysics, **vol.** 155, August 2018, pp. 131-137.

[2]. *R. Streich*, "Controlled-Source Electromagnetic Approaches for Hydrocarbon Exploration and Monitoring on Land," Surveys in Geophysics, **vol.** 37, no. 1, 2016, pp. 47-80,

[3]. *M. Chongo, A.* Vest Christiansen, A. Tembo, K. E. Banda, I. A. Nyambe, and F. Larsen, et al., "Airborne and ground-based transient electromagnetic mapping of groundwater salinity in the Machile–Zambezi Basin, southwestern Zambia," Near Surface Geophysics. **vol.** 13, no. 4, 2015, pp. 383-396.

[4]. *X. Li, Z.P. Qi, G.Q. Xue, et al.* Three-dimensional curved surface continuation image based on TEM pseudo wave-field. Chinese J. Geophysics. **vol.** 53, no. 12, 2010, pp. 3005-3011.

[5]. *Z.P. Qi, Li X, Q. Wu, et al.* Inverse transformation algorithm of transient electromagnetic field and its high-resolution continuous imaging interpretation. Chinese J. Geophysics. **vol.** 56, no. 10, 2015, pp. 3581-3595.

[6]. *G. Kunetz,* "Processing and interpretation of magnetotelluric soundings," Geophysics, **vol.** 37, no. 6, 1972, pp. 1005-1021.

[7]. *Lavrent'ev M M, Romanov V G, Shishatskii S P.* Ill-posed Problems of Mathematical Physics and Analysis. Providence RI:American Mathematical, 1986.

[8]. *K.H. Lee, G. Liu, H.F. Morrison.* A new approach to modeling the electromagnetic response of conductive media. Geophysics. **vol.** 54, no. 9, 1989, pp. 1180-1192.

[9]. *B.C. Chen, J.M. Li, F.T. Zhou.* Wave-field transformation algorithm for transient electromagnetic field. OGP, **vol.** 34, no. 5, 1999, pp. 539-545.

[10]. *X. Li, G.Q. Xue, J. P. Song, et al.* An optimize method for transient electromagnetic field-wave field conversion. Chinese J. Geophysics. **vol.** 48, no. 5, 2005, pp. 1185-1190.

[11]. *Z.P. Qi, X. Li, Q. Wu, et al.* A new algorithm for full-time-domain wave-field transformation based on transient electromagnetic method. Chinese J. Geophysics. **vol.** 56, no. 10, 2013, pp. 3581-3595.

[12]. *Y.J. Ji, Y.P.* Hu, and Imamura N, Three-Dimensional Transient Electromagnetic Modeling Based on Fictitious Wave Domain Methods, Pure and Applied Geophysics, **vol.** 174, no. 5, 2017, pp. 2077-2088.

[13]. *J.G. Hu,* Linear Algebraic Equations Iterative Methed, Beijing; Science press, 1991.

[14]. *Z.Z. Bai,* A class of modified block SSOR preconditioners for symmetric positive definite systems of linear equations, Advances in Computational Mathematics, **vol.** 10, 1999, pp. 169-186.

[15]. *Z.Z. Bai,* A regularized conjugate gradient method for symmetric positive definite systems of linear equations, Advances in Computational Mathematics, **vol.** 20, no. 4, 2002, pp.437-448.

[16]. *F. Yan, C.L. Fu, X.X. Li,* A modified tikhonov regularization method for the cauchy problem of laplace equation, Acta Mathematica Scientia, **vol.** 35B, no. 6, 2015, pp. 1339–1348.

[17]. *X.J. Yan, L. Wang,* A modified Tikhonov regularization method, Journal of Computational and Applied Mathematics, **vol.** 288, 2015, pp. 180–192.